JOURNAL OF APPLIED POLYMER SCIENCE VOL. 19, PP. 2299–2308 (1975)

Flow Properties of ABS (Acrylonitrile–Butadiene–Styrene) Terpolymer

HIDEO KUBOTA,* *General Motors Research Laboratories, Warren, Michigan 48090*

Synopsis

ABS (acrylonitrile–butadiene–styrene) terpolymer is a two-phase thermoplastic with SAN (styrene–acrylonitrile) copolymer constituting the continuous phase (matrix). The flow properties of ABS with varying molecular parameters were studied using a capillary viscometer at the shear rate range encountered in its processing. The viscosity-average molecular weights (M_v) of matrix SAN with 26% acrylonitrile content are in the range of 90,000 to 150,000, and M_v of polybutadiene are in the range of 150,000 to 170,000. The weight-average molecular weight of the matrix SAN is the main controlling factor for the flow properties of ABS at low shear rate, while the molecular weight distribution of the matrix SAN becomes increasingly important with the increase of shear rate. The presence of SAN grafted polybutadiene increases the melt viscosity of ABS by 40–60% over comparable free SAN copolymer and also decreases the activation energy at constant shear stress to 24–25 kcal/mole from the 33–36 kcal/mole for free SAN. The die swell of ABS and SAN can be correlated with the dynamic shear modulus G', and the melt fracture of ABS and SAN starts at G' equal to 3.6×10^6 dynes/cm^2.

INTRODUCTION

ABS (acrylonitrile–butadiene–styrene) terpolymer is fabricated mainly by melt processing, and its processing characteristics depend upon the flow properties at processing temperatures. ABS is a two-phase thermoplastic, in which SAN (styrene–acrylonitrile) copolymer constitutes the continuous phase (matrix) and polybutadiene constitutes the dispersed phase. Therefore, the flow properties of ABS are affected by more than one structural parameter in this plastic, i.e., those of matrix and dispersed phase polymers. This paper reports the effects of some of these structural parameters on the melt flow properties in a wide range of shear rate as experienced in various types of melt processing.

EXPERIMENTAL

Analysis of Materials

The three styrene–acrylonitrile copolymers (SAN) studied by rheometry have an acrylonitrile content of 26.0%. The average molecular weight of these copolymers was determined by gel permeation chromatography (GPC) and by intrinsic viscosity.

The chemical composition of ABS was analyzed by the following method[1]:

* Present address: Hooker Research Center, Long Road, Grand Island, New York 14072.

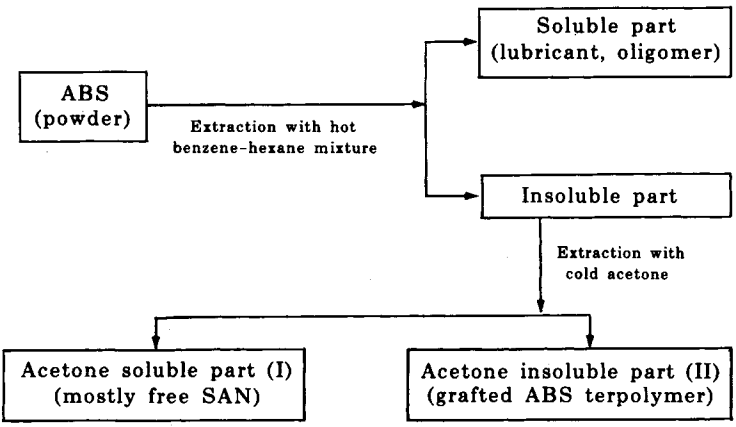

The acetone-soluble part (I) of ABS is considered to be SAN copolymer because no polybutadiene can be dissolved in acetone at room temperature. However, the infrared spectra of the acetone-soluble part (I) showed a weak absorption at 10.3 μ, which is attributed to trans—CH=CH— structure of polybutadiene and also weak absorptions at 6.1 μ and 10.1 μ, both of which are due to CH_2=CH— structure of polybutadiene. These results indicate that even the acetone-soluble part (I) contains a small amount of free and/or grafted polybutadiene. The molecular weight of (I) was determined by GPC and by intrinsic viscosity. GPC also provided information on the molecular weight distribution.

The acetone-insoluble part (II) consists of the grafted ABS terpolymer. After II was swelled in hot toluene (100°C) with a trace of formic acid, ozone was introduced into this swollen gel for 4 hr. Ozone caused the breakage of the double bonds of the polybutadiene, and one of the reaction products was linear SAN. The resultant SAN was extracted with tetrahydrofuran and the molecular weight of this SAN was determined by GPC and intrinsic viscosity.

Measurement of Flow Properties

A capillary rheometer was used for the measurement of the flow properties of SAN and ABS. The shear stress at the wall of a capillary, τ_w, was calculated by eq. (1):

$$\tau_w = \frac{R\Delta P}{2L\left(1 + e\frac{R}{L}\right)} \tag{1}$$

where P = frictional pressure drop; L = length of a capillary; R = radius of a capillary; and e = end correction factor.

The end correction factor e was determined from the frictional pressure drop through the capillaries with different ratios of L/R but constant R. It was found that e is independent of shear rate in the low shear rate range of less than 100 sec^{-1}, but dependent on the shear rate at a higher shear rate range of more than 500 sec^{-1}.

The shear rate at the wall of a capillary, $\dot{\gamma}$, was calculated by the Rabinowitsch-Mooney equation,[2,3] equation (2):

$$\dot{\gamma} = \left(\frac{3n + 1}{4}\right)\frac{4V}{R} \tag{2}$$

where V is the average linear velocity and n is defined by

$$n = \frac{d \ln (R\Delta P/2L)}{d \ln (4V/R)} . \tag{3}$$

Although there are many approaches to the elastic factor in capillary flow,[4] dynamic shear modulus[5,6] G' defined in eq. (4) was related to the relative die swell of extrudate:

$$G' = \dot{\gamma}(\eta_a^2 - \eta^2)^{1/2} \tag{4}$$

where η_a is apparent viscosity defined by $\eta_a = \tau_w/\dot{\gamma}$ and η is consistency defined by $\eta = (d\tau_w/d\dot{\gamma})$. The relative die swell is $(D/D_0 - 1)$, where D is the diameter of extrudate and D_0 is the diameter of a capillary.

RESULTS AND DISCUSSION

ABS consists of three polymeric components: (1) SAN copolymer, (2) polybutadiene on which SAN copolymers are grafted, and (3) pure polybutadiene. The grafted polybutadiene, providing the link between the dispersed rubber phase and the rigid continuous SAN phase, contributes to the toughness and impact strength of ABS, while matrix SAN contributes to the rigidity and dimensional stability of ABS. Since SAN forms the matrix of ABS and occupies more than half of the volume of ABS, the molecular parameters of the SAN in ABS, i.e., acrylonitrile/styrene ratio, average molecular weight, and molecular weight distribution, strongly affect the flow properties of ABS. Therefore, knowledge of the flow properties of SAN is a prerequisite for the elucidation of the flow properties of ABS.

Flow Properties of SAN

The acrylonitrile content of the three SAN copolymers studied is 26.0%, which is the same as the acrylonitrile content of the SAN in ABS. Figure 1 shows the shear rate-versus-shear stress relationship of these copolymers. SAN-1 and SAN-3 have approximately the same molecular weight distribution as shown by the ratio of M_w/M_n, where M_w is the weight-average molecular weight and M_n is the number-average molecular weight. M_v is the viscosity-average molecular weight obtained from the intrinsic viscosity. The difference of the flow curves between SAN-1 and SAN-3 can be explained by the molecular weight difference between these SAN. However, the similarity of the flow curves at high shear rate between SAN-2 and SAN-3 cannot be explained by the molecular weights of SAN-2 and SAN-3. In fact, the flow curves of SAN-2 and SAN-3 are practically the same at 5000 sec^{-1} or higher, in spite of the fact that SAN-2 has a higher M_w than SAN-3. This marked decrease in the shear stress of SAN-2 at high shear rate, so-called shear thin-

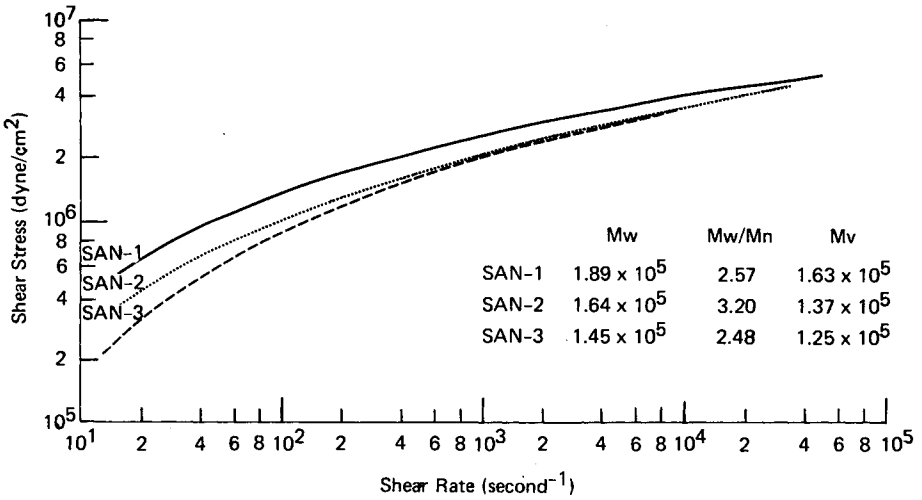

Fig. 1. Shear stress vs. shear rate relationship for SAN at 220°C.

ning, is attributed to the wider molecular weight distribution of SAN-2. At high shear rate, the molecular weight distribution becomes more of a controlling factor for the flow properties than the average molecular weight.

Flow Properties of ABS

Since ABS consists of three polymeric components, the molecular parameters of ABS should be identified in terms of these three components. Table I shows the results of the chemical analysis of the ABS. Although we could not determine the molecular weights of polybutadiene in ABS, it was inferred that the initiation M_w of polybutadiene used for preparation of the ABS are in the range of 1.5×10^5 to 1.7×10^5.

ABS-1 is an extrusion-grade ABS with high impact strength, 8.5 ft-lb/in., and low modulus, 27,000 psi, while ABS-3 is in injection molding-grade resin

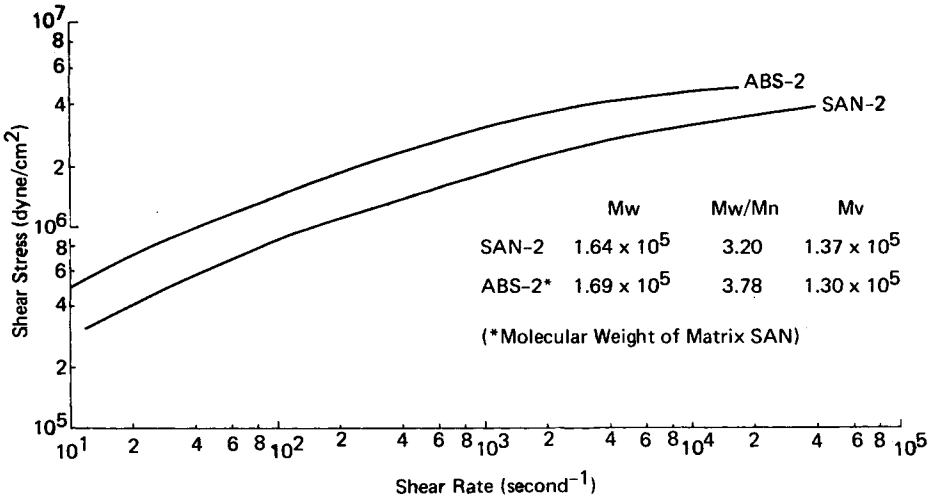

Fig. 2. Shear stress vs. shear rate relationship for ABS and SAN at 240°C.

TABLE I
Chemical Composition and Molecular Parameters of ABS[a]

Material designation	Acetone-soluble part, %	Acetone-insoluble part, %	Acetone-soluble part			Acetone-insoluble part M_w
			M_w	M_w/M_n	M_v	
ABS-1	78.1	20.1	2.02×10^5	5.8	1.5×10^5	7×10^4
ABS-2	77.2	21.4	1.69×10^5	3.8	1.3×10^5	7×10^4
ABS-3	74.0	25.3	1.18×10^5	4.5	$.9 \times 10^5$	10×10^4

[a] M_n = Number-average molecular weight; M_w = weight-average molecular weight; M_v = viscosity-average molecular weight.

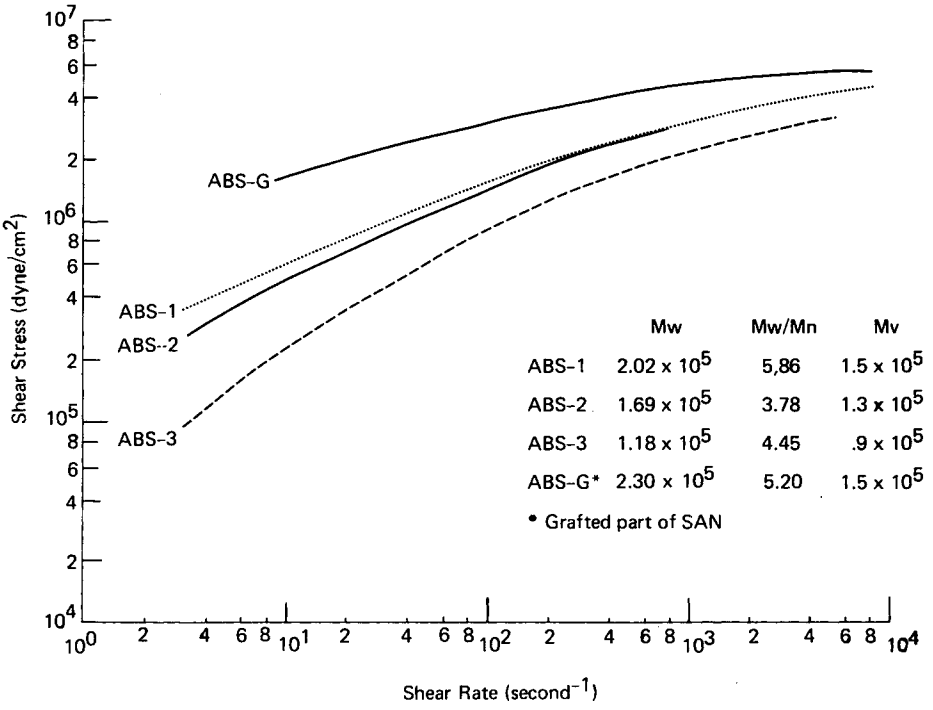

Fig. 3. Shear stress vs. shear rate relationship for ABS at 240°C.

with relatively low impact strength, 5.0 ft-lb/in., and medium modulus, 320,000 psi. ABS-2 is a medium impact-strength (7.0 ft-lb/in.) resin with a high tensile strength.

Figure 2 compares the flow curve of SAN with the flow curve of ABS. The M_w of SAN-2 is almost the same as the M_w of the SAN in ABS-2. At low shear-rate range, where the molecular weight distribution does not greatly affect the flow curve, the presence of the grafted polybutadiene causes an increase of 60% of the shear stress of SAN-2 as shown in Figure 2.

Although the M_w is the same for SAN-2 and ABS-2, the molecular weight distribution of SAN-2 is narrower than the molecular weight distribution of the acetone-soluble part of ABS-2, as evidenced by the ratio of M_w/M_n in Figure 2. It was found that the molecular weight distribution of the matrix SAN in ABS is generally wider than that of SAN copolymer. Since the wide molecular weight distribution causes stronger shear thinning at the high shear rate as discussed earlier, the flow curve of ABS-2 is expected to have

stronger shear thinning than the flow curve of SAN-2. The shear stress of ABS-2 is approximately 60% higher than the shear stress of SAN-2 at low shear rates of less than 100 sec^{-1}; and the shear stress of ABS-2, despite stronger shear thinning, is approximately 40% higher than the shear stress of SAN-2 at high shear rates of more than 4000 sec^{-1}. These differences in the shear stress between ABS-2 and SAN-2 are attributable to the presence of SAN-grafted polybutadiene in ABS.

Figure 3 shows the flow curves of four types of ABS. The difference in the flow curves at the low shear rate among these ABS can be explained by the difference in M_w of the matrix SAN in these ABS. However, the molecular weight distribution of the matrix SAN becomes the controlling factor on the flow properties at the high shear rate. The flow curves of ABS-1 and ABS-2 become similar at 1000 sec^{-1} or higher, despite the lower M_w of the matrix SAN of ABS-2 as shown in Figure 3. This is because ABS-1 has the wider molecular weight distribution of matrix SAN than ABS-2, as shown in Table I.

ABS-G, a specially prepared ABS with an extremely high degree of SAN grafting, has a very high viscosity compared to the other three ABS. More than 60% of the SAN in ABS-G is grafted to the polybutadiene which has the viscosity-average molecular weight of 1.5×10^5. ABS-G has a very high impact strength, 12.5 ft-lb/in. A high degree of grafting in ABS, though it enhances the impact strength of ABS, increases the melt viscosity of ABS. Therefore, the degree of grafting is another controlling factor on the flow properties of ABS.

The Temperature Dependence of Melt Viscosity

The temperature dependence of melt viscosity, η, is generally expressed in terms of activation energy E in the Arrhenius-type equation

$$\eta = \eta_0 \exp(E/RT) \tag{6}$$

where R is the gas constant and T is the absolute temperature. Unlike the viscosity of Newtonian liquids, where η is a unique function of T, the viscosity of non-Newtonian liquids cannot be a unique function of T, but a function of T and either shear stress τ_w or shear rate $\dot{\gamma}$. Therefore, two different activation energies can be defined: (1) activation energy at constant shear stress E_{τ_w}:

$$E_{\tau_w} = -R\left(\frac{\delta \ln \eta}{\delta(1/T)}\right)_{\tau_w = \text{constant}}$$

and (2) activation energy at constant shear rate $E_{\dot{\gamma}}$:

$$E_{\dot{\gamma}} = -R\left(\frac{\delta \ln \eta}{\delta(1/T)}\right)_{\dot{\gamma} = \text{constant}}$$

Although E_{τ_w} and $E_{\dot{\gamma}}$ differ from each other, they should merge at zero shear:

$$\lim_{\tau_w \to 0} E_{\tau_w}(\tau_w) = \lim_{\dot{\gamma} \to 0} E_{\dot{\gamma}}(\dot{\gamma}) = E. \tag{7}$$

TABLE II
Activation Energy at Constant Shear Stress, E_{τ_w}, for SAN and ABS

Shear stress, dynes/cm²	E_{τ_w} for SAN-3[a] kcal/mole	E_{τ_w} for ABS-3[b] kcal/mole
5.0×10^5	33.0	23.8
8.0×10^5	34.4	24.0
10.0×10^5	35.3	24.4
20.0×10^5	36.0	24.8

[a] Temperature range = 190°—240°C.
[b] Temperature range = 220°—260°C.

TABLE III
Activation Energy at Constant Shear Rate, $E_{\dot{\gamma}}$, for SAN and ABS

Shear rate, sec⁻¹	$E_{\dot{\gamma}}$ for SAN-3,[a] kcal/mole	$E_{\dot{\gamma}}$ for ABS-3,[b] kcal/mole
3.0	21.0	20.0
15.0	15.2	17.0
29.9	12.8	15.2
149.0	9.9	10.8
299.0	9.0	9.0
746.0	8.7	8.3
1490.0	8.4	6.2
5750.0	—	2.5

[a] Temperature range = 190°—240°C.
[b] Temperature range = 220°—260°C.

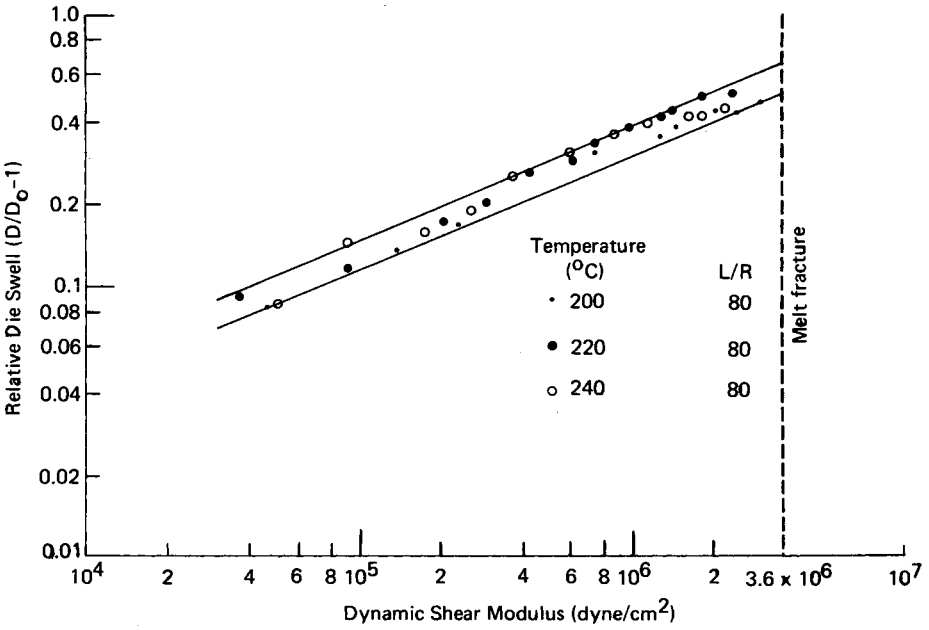

Fig. 4. Relative die swell vs. dynamic shear modulus relationship for SAN.

Since the activation energy is independent of the molecular weight above the critical molecular weight, $E\tau_w$ and $E\dot{\gamma}$ for only one SAN and ABS are shown in Tables II and III. Extrapolation of the activation energy of SAN to zero shear stress yields 32.2 kcal/mole for E defined in eq. (7). Compared with E of polyethylene,[7] 7.0 kcal/mole, and polystyrene,[8] 21.2 kcal/mole, E of SAN is very high, which is attributed to the high cohesive energy of acrylonitrile pendent group, —C≡N. Table III also shows that $E\dot{\gamma}$ strongly depends on the shear rate. At the shear rates of higher than 5000 sec^{-1}, where injection molding usually operates, the viscosity fluctuation due to the temperature is minimal. The E of ABS is about 24.0 kcal/mole, which is much smaller than E for SAN.

Melt Elasticity of ABS and SAN

The elastic properties of polymer melt are of great importance for polymer processing. There are several theories[9–12] which relate die swell with the elasticity of polymer melts. One of them, the theory by Philippoff and Gaskins,[9] proposed that the end correction factor e in eq. (1) could be expressed by the following equation:

$$e = N + \frac{1}{2}S_R \tag{8}$$

where N, Couette correction, is the correction which would arise from the viscous loss upstream of the capillary entrance; and S_R, recoverable shear, is the elastic correction which would arise from the recoverable deformation im-

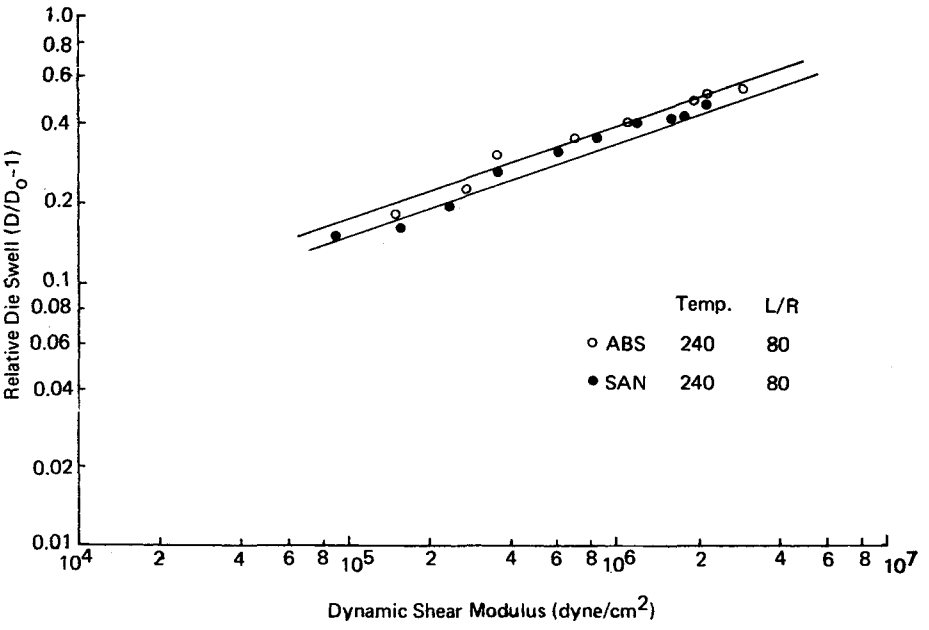

Fig. 5. Relative die swell vs. dynamic shear modulus relationship for ABS and SAN at 240°C.

posed on the melt at the entrance of a capillary. Philippoff and Gaskins[9] claimed that S_R is related to the postextrusion die swell as well as the normal force of the extrudate. If so, dynamic shear modulus rather than the shear stress should correlate with the die swell under different conditions.

In Figure 4, the relative die swell, $D/(D_0 - 1)$, which is a function of both the temperature and the shear stress (or shear rate), is plotted against dynamic shear modulus G', defined by eq. (5). Figure 4 shows that the relative die swell at different temperatures can be clearly correlated by a unique function of G', and the melt fracture of SAN (in the capillary with L/R ratio of 80 and R of 0.05 in.) started at the following shear rate and temperature:

Temperature (°C)	Critical Shear Rate (second^{-1})
180	224
220	1,780
240	4,500

At all these shear rates, G' becomes 3.6×10^6 dynes/cm^2. The same relationship holds for the die swell of ABS (Fig. 5). Here again, the critical shear rate of all three ABS falls to one value of G', 3.6×10^6 dynes/cm^2:

Material Designation	Critical Shear Rate at 240°C In Capillary With L/R Ratio of 80 (second^{-1})
ABS-1	1,250
ABS-2	1,270
ABS-3	450

It was also found that the die swell of ABS is slightly larger than the die swell of SAN at the same temperature and shear rate. With ABS, the molecular parameters of matrix SAN mainly determine the dynamic shear modulus and thus the elasticity of ABS.

Flow Properties and Structural Parameters of ABS

The results discussed so far lead to several important conclusions on the structural effects of ABS on the flow properties:

1. The molecular weight and molecular weight distribution of matrix SAN primarily control the flow properties of ABS. The wider molecular weight distribution of matrix SAN causes greater shear thinning.
2. The presence of grafted polybutadiene in ABS greatly increases the melt viscosity of ABS compared to the melt viscosity of SAN with similar molecular parameters of the matrix SAN in ABS.
3. The melt elasticity of ABS, slightly larger than that of SAN at the same temperature and shear rate, is controlled by the matrix SAN in ABS.

The physicomechanical properties of ABS are also affected by these parameters. For example, the high impact strength of ABS is inherently associated with the high molecular weight of dispersed rubber having a low glass transition temperature[13] and a high degree of grafting of SAN.[14] The high degree of grafting and, to a lesser extent, the high molecular weight of rubber

obviously increase the melt viscosity of ABS and thus contribute to the difficulty of processing. Narrow molecular weight distribution usually contributes to an increase in the impact strength and an increase in the melt viscosity at high shear rate. Increase in the rubber content and decrease in the degree of grafting may result in low melt viscosity and high impact strength but only with the sacrifice of other important properties such as rigidity. Introduction of a rigid monomer such as acenaphthalene in the matrix to compensate for these sacrificed properties inevitably depresses impact strength[13] and increases the melt viscosity. Therefore, a possible approach to resolving this dilemma is the development of a viscosity modifier which does not adversely affect the mechanical properties at service temperature.[15]

References

1. L. D. Moore and W. J. Frazer, *Prepr. Amer. Chem. Soc.* (Organic Coating and Plastics), **27**, 313 (1967).
2. B. Rabinowitsch, *Z. Phys. Chem.*, **A145**, 1 (1929).
3. M. Mooney, *J. Rheol.*, **2**, 210 (1931).
4. C. D. Han, *Trans. Soc. Rheol.*, **18**, 163 (1974).
5. Y. Pao, *J. Appl. Phys.*, **28**, 591 (1957).
6. W. P. Cox and H. E. Merz, *J. Polym. Sci.*, **28**, 619 (1958).
7. R. S. Porter and J. F. Johnson, *J. Polym. Sci.*, **C15**, 375 (1966).
8. R. S. Porter and J. F. Johnson, *J. Polym. Sci.*, **C15**, 365 (1966).
9. W. Philippoff and F. H. Gaskins, *Trans. Soc. Rheol.*, **2**, 263 (1958).
10. T. Arai and H. Aoyama, *Trans. Soc. Rheol.*, **7**, 333 (1963).
11. B. D. Coleman and W. Nolly, *Ann. New York Acad. Sci.*, **23**, 672 (1961).
12. E. B. Bagley, S. H. Storey, and D. C. West, *J. Appl. Polym. Sci.*, **7**, 1661 (1963).
13. E. M. Hagerman, *J. Appl. Polym. Sci.*, **13**, 1873 (1969).
14. V. K. Dignes and H. Schuster, *Makromol. Chem.*, **101**, 200 (1967).
15. H. Kubota, U.S. Pat. 3,624,182 (1971).

Received October 17, 1974
Revised December 16, 1974